FOLIA HISTOCHEMICA ET CYTOBIOLOGICA
Vol. 60, No. 3, 2022
pp. 260–270

ORIGINAL PAPER

VIA MEDICA

HDAC5 inhibits ovarian angiogenesis in dehydroepiandrosterone-induced mouse model of polycystic ovary syndrome

Ying Wang[1], Yu Wang[2], Yao Chen[2], Qianqian Gao[2], Lihui Hou[1], Xiaoling Feng[1]

[1]The Second Department of Gynecology, First Affiliated Hospital, Heilongjiang University of Chinese Medicine, Harbin, China

[2]Graduate School, Heilongjiang University of Chinese Medicine, Harbin, China

Abstract

Introduction. Abnormal ovarian angiogenesis is a common feature of polycystic ovary syndrome (PCOS), a typical endocrine disorder affecting women of reproductive age. Histone deacetylase 5 (HDAC5) has been documented as a suppressor of angiogenesis. The aim of this study was to explore the effect of HDAC5 on ovarian angiogenesis in a PCOS mouse model.

Material and methods. PCOS was induced in female C57BL/6 mice by 20-day administration of dehydroepiandrosterone (DHEA). HDAC5 was over-expressed in PCOS mice by corresponding adenovirus injection. In total, 120 mice were used in this study. Western-blotting, real-time PCR, hematoxylin and eosin staining, enzyme-linked immunosorbent assay (ELISA), immunohistochemical staining, flow cytometry, and co-immunoprecipitation were respectively used to evaluate the effect of HDAC5 on PCOS mice.

Results. PCOS ovaries showed a compensatory increase in HDAC5 expression, while HDAC5 over-expression alleviated abnormalities in ovarian morphology and serum hormone levels after PCOS modeling. HDAC5 inhibited ovarian angiogenesis in PCOS mice by regulating angiogenesis-related factors, such as VEGFA, platelet-derived growth factors B and D (PDGFB/D), and angiopoietins 1 and 2 (ANGPT1/2) and CD31. HDAC5 over-expression decreased levels of reactive oxygen species (ROS) and malondialdehyde, while promoting activities of catalase and superoxide dismutase in ovaries of PCOS mice, suggesting its suppressive effects on oxidative stress, an inducer of uncontrolled angiogenesis. Moreover, HDAC5 suppressed activation of angiogenesis-related HIF-1α/VEGFA/VEGFR2 signaling in PCOS ovaries partly *via* inhibiting VEGFR2 acetylation.

Conclusions. This study reveals the protective role of HDAC5 in PCOS by inhibiting ovarian angiogenesis and provides a molecular candidate for PCOS therapy in the future. *(Folia Histochemica et Cytobiologica 2022, Vol. 60, No. 3, 260–270)*

Keywords: mouse; polycystic ovary syndrome; HDAC5 overexpression; angiogenesis; oxidative stress

Corresponding authors:
Prof. Xiaoling Feng
The Second Department of Gynecology, First Affiliated Hospital, Heilongjiang University of Chinese Medicine, No. 26, Heping Road, Harbin, China
e-mail: doctorfxl@163.com
Prof. Lihui Hou
The Second Department of Gynecology, First Affiliated Hospital, Heilongjiang University of Chinese Medicine, No. 26, Heping Road, Harbin, China
phone: +86-451-82111401
e-mail: houlihui2007@sina.com

Introduction

Polycystic ovary syndrome (PCOS) is the most common endocrine and metabolic disorder that affects women of reproductive age [1]. Clinically, PCOS is characterized by excessive androgen secretion, ovulation failure, and pathological ovarian changes. Although the pathogenesis of PCOS has not been fully explored, it is documented to associate with obesity, insulin resistance, and dyslipidemia [1, 2]. More importantly, PCOS patients are more likely to

Folia Histochem Cytobiol. 2022
10.5603/FHC.a2022.0024
ISSN 0239-8508, e-ISSN 1897-5631

www.journals.viamedica.pl/folia_histochemica_cytobiologica

have long-term complications, such as hyperlipidemia, cardiovascular disorder, hypertension, and endometrial cancer, which makes PCOS a critical health concern for women worldwide [3].

Recently, ovarian angiogenesis has been proved as an interesting field for PCOS research [4, 5]. As the key organ of the female reproductive system, the ovary represents one of the few organs with active angiogenesis. The accurate formation and regression of blood vessels play an indispensable role in follicular development, ovulation, and corpus luteum generation, which are crucial events in the reproductive system cycle [4]. Of note, altered ovarian angiogenesis is a common feature in PCOS. Patients with PCOS have displayed an obviously higher level of angiogenesis when compared to healthy women [6]. Besides, significantly promoted angiogenic effects have been determined in ovaries of PCOS rats [5, 7], which further suggests that ovarian angiogenesis is a promising therapeutic target for PCOS.

Histone deacetylase 5 (HDAC5) is a crucial member of the class II HDAC family, which could affect gene transcription by regulating acetylation and chromatin remodeling [8]. It has shown prominent roles in a broad array of biological processes and is associated with a pathological state of many disorders [9]. For instance, HDCA5 exerts suppressive effects on tumor cell proliferation in neuroblastoma and breast cancer [10, 11]. HDAC5 was shown to promote inflammation in a mouse model of intestinal sepsis [12]. However, the role of HDCA5 in PCOS has not been explored yet. Inspiringly, HDAC5 has been documented as an angiogenesis repressor in endothelial cells [13], which suggests that HADC5 might be involved in ovarian angiogenesis during PCOS progression.

Oxidative stress manifested as the imbalance between pro- and anti-oxidant systems plays a key role in angiogenesis. It is well-established that oxidative stress could result in numerous vascular-related diseases [14]. More importantly, women with PCOS presented higher indices of oxidative stress when compared to non-PCOS individuals, validating the involvement of oxidative stress in PCOS pathogenesis [15]. It is worthy to note that HDAC5 has the property to regulate oxidative stress in cerebral ischemia and cardiac hypertrophy [16, 17]. Additionally, oxidative stress-induced angiogenesis is strongly associated with the accumulation of reactive oxygen species (ROS) and the activation of hypoxia-inducible factor-1alpha (HIF-1α)/vascular endothelial growth factor (VEGF) signaling [14, 18]. Thus, this study aimed to explore whether HDAC5 over-expression in PCOS mice inhibits ovarian angiogenesis, and investigate the potential associations between HDAC5 expression and ROS/ /HIF-1α/VEGF signaling in PCOS.

Materials and methods

Animals. Female C57BL/6 mice (21-day old, 9–13 g) were housed in a specialized facility with a temperature of 22 ± 1°C, the humidity of 45–55%, and a 12-h day/night cycle. Mice were adaptively kept for one week with free access to water and food prior to PCOS modeling. In total, 120 mice were used in this study. All animal experimental protocols were approved by the Animal Care and Use Committee of Heilongjiang University of Chinese Medicine (Approval number: 2021111103).

PCOS modeling and interventions. Female C57BL/6 mice were randomly divided into 4 groups after one-week accommodation (n = 6 in each group), *i.e.* control, PCOS, PCOS + Ad-vector, and PCOS + Ad-HDAC5 groups. PCOS mice received a daily subcutaneous injection of dehydroepiandrosterone (DHEA, 60 mg/kg, dissolved in sesame oil, Aladdin Reagent, Shanghai, China) for continuous 20 days [19]. Meanwhile, control mice were injected with the same volume of solvent. One week prior to PCOS modeling, mice in adenovirus-treated groups received the injection of adenovirus expressing HDAC5 and an empty vector (3×10^9 PFU/ovary, 10 μL, in DMEM) at the position below ovary capsule. HDAC5 over-expression *in vivo* was achieved by adenovirus administration.

To construct the recombinant adenovirus expressing HDAC5, the segment of HDAC5 was synthesized, and cloned into the pShuttle-CMV vector (Fenghui Biotechnology, Hunan, China). The plasmid was validated by enzyme digestion and DNA sequencing. Recombinant adenovirus expressing HDAC5 was subsequently generated using the classical AdEasy system [20]. After the measurement of virus titer, the *in vivo* transduction with the indicated amount of adenovirus expressing HDAC5 was performed on mice, and the transduction efficiency was determined by detecting HDAC5 expression in ovarian tissues from experimental mice using western-blot and real-time PCR. On day 21 post first DHEA injection, the animals were anesthetized with sevoflurane, and blood was taken from the retroorbital venous plexus of animals until their death. Thereafter, ovarian tissues were collected for further analysis.

Hematoxylin and eosin (H&E) staining. After fixation in 10% buffered formalin for over 24 h at room temperature (RT), ovarian tissues underwent conventional dehydration, paraffin-embedding, and sectioning (5 μm-thick). Sections were then air-dried and dewaxed prior to the staining with hematoxylin (H8070, Solarbio, Beijing, China) and eosin (A600190, Sangon Biotech, Shanghai, China) according to the established protocol [21]. Representative microphotographs of ovaries were captured using a light microscope (Olympus, Tokyo, Japan) at the magnification of 40×.

Immunohistochemistry. Ovary sections from each group were fixed and paraffin-embedded as described for H&E staining. For immunohistochemical (IHC) staining, prepared

5 μm-thick sections were incubated with boiled citrate antigen retrieval solution (PH = 9) for 10 min and then immersed into 3% H_2O_2 (10011218, Sinopharm, Beijing, China) for 15 min. Subsequently, sections were blocked by 1% bovine serum albumin (BSA, A602440-0050, Sangon Biotech, Shanghai, China) for 15 min at RT and then incubated with primary antibody against CD31 (1:50, AF6191, Affinity, Jiangsu, China) at 4°C overnight. The allotypic serum was used as a control to determine the specificity of CD31 staining. On the following day, sections were incubated with secondary antibody (1:500, #31460, ThermoFisher, Waltham, MA, USA) for 60 min at 37°C. After washing, slides were further stained with diaminobenzidine (DAB, DAB-1031, MXB Biotechnology, Foochow, China) and lightly counterstained with hematoxylin (H8070, Solarbio). After dehydration and mounting, sections were finally analyzed using a light microscope (Olympus).

Enzyme-linked immunosorbent assay (ELISA). Whole blood taken from retroorbital venous plexus (approximately 1 mL/ /mouse) was collected in a test tube without anticoagulant and left to clot for 4 h at RT and then was subjected to centrifugation at 4°C for 10 min at 3000 rpm. The supernatant was taken as the serum (about 500 μL/mouse). The serum levels of progesterone, testosterone, and estradiol were detected using ELISA kits (EU0398, EU0400, EU0390, respectively, Finetest, Wuhan, China).

The bicinchoninic acid (BCA) assay was performed to quantify protein concentrations in supernatants derived from ovarian tissue homogenates. For homogenization, indicated volume of normal saline (pH 7.0) was added to tissue samples at the ratio of 9:1 (volume: tissue weight). The samples were homogenized using a hand-held glass homogenizer in baths of ice. Supernatants derived from tissue homogenates were next obtained by centrifugation at 4°C for 10 min at 2500 rpm. ELISA was subsequently performed to detect concentrations of vascular endothelial growth factor A (VEGFA, EK283, MULTI Sciences, Hangzhou, China), angiopoietin 1 (ANGPT1, EM0016, FineTest), angiopoietin 2 (ANGPT2, EM0017, FineTest), platelet-derived growth factor-B (PDGFB, EM0269, FineTest) and platelet-derived growth factor-D (PDGFD, EM1271, FineTest) in supernatants of homogenized ovarian tissues by commercial ELISA kits.

ROS detection *via* flow cytometry. Ovarian tissue was made into single-cell suspension using established protocol [22]. Afterward, cells were probed with dichloro-dihydro-fluorescein diacetate (DCFH-DA,10 μM) for 20 min at 37°C according to the manufacturer's instructions (S0033S, Beyotime). After the removal of excess DCFH-DA, cells were subjected to the flow cytometric analysis (NovoCyte, Agilent, Santa Clara, CA, USA).

Biochemical analysis. Protein extracts in supernatants of homogenized ovarian tissues were quantified by commercially available BCA assay kit (P0011, Beyotime). To detect malondialdehyde (MDA) level, the protein concentration of each sample was unified to 1 mg/mL, and protein samples were subsequently subjected to thiobarbituric acid (TBA) assay using commercial assay kit (A003-1) from Nanjing Jiancheng Bioengineering Institute (Nanjing, China). The absorbance at 532 nm was measured by a spectrophotometer (UV752N, UNICO, Shanghai, China), and MDA level was expressed as nmol/mg protein according to the manufacturer's protocol.

The activity of catalase (CAT) in homogenate samples (protein concentration was unified to 2 mg/mL) was detected using a CAT assay kit (A007, Nanjing Jiancheng Bioengineering Institute) by measuring absorbance at 405 nm. CAT activity was expressed as U/mg protein according to the manufacturer's protocol.

Superoxide dismutase (SOD) activity in supernatants of homogenized ovarian tissues (protein concentration was unified to 1 mg/mL) was detected by hydroxylamine method using commercial assay kit (A001) from Nanjing Jiancheng Bioengineering Institute. The absorbance at 550 nm was measured, and SOD activity was expressed as U/mg protein according to the manufacturer's protocol.

Real-time PCR. Total RNA was isolated from ovarian tissue by TRIpure buffer (RP1001, BioTek, Beijing, China). Isolated RNAs were reversed into cDNAs using BeyoRT II M-MLV reverse transcriptase (D7160L, Beyotime) on a PCRAmplifier (TC-96/G/H(b), Bioer Technology, Hangzhou, China). The Reverse Transcription System was listed as follows:

Step 1: prepare a 12.5 μL reaction by adding 1 μg RNA, 1 μL oligo $(dT)_{15}$, 1 μL random primers, and ddH_2O. The reaction was incubated at 70°C for 5 min, then placed on ice for 2 min;

Step 2: 2 μL dNTP, 4 μL 5× buffer, 0.5 μL Rnase inhibitor, and 1 μL M-MLV reverse transcriptase were added into reaction. The total reaction samples were then incubated at 25°C for 10 min, 40°C for 50 min, and 80°C for 10 min.

cDNAs were then subjected to the real-time PCR analysis together with SYBR green (SY1020, Solarbio) and corresponding primers. Relative expressions of the target genes were normalized to β-actin gene expression and analyzed by the $2^{-\Delta\Delta CT}$ method [23]. Primers used in this study were provided as follows: HDAC5 F: TCTCCGCTGGGTTTGAT; HDAC5 R: ATTGACGCTGGGCTTTT; VEGFA F: CTACTGCCGTCCGATTGAG; VEGFA R: CTGGCTTTGGTGAGGTTTG; HIF-1α F: GTATTATTCAGCACGACTT; HIF-1α R: GAGGGAAACATTACATCA; VEGFR2 F: TTTTGAGCACCTTGACA; VEGFR2 R: GGGATTCGGACTTGACT.

Measurements of protein contents by Western blotting. To obtain ovarian protein extracts, ovarian tissues was lysed by radioimmunoprecipitation assay (RIPA) lysis buffer (P0013B, Beyotime) containing 1% phenylmethylsulfonyl fluoride (PMSF, ST506, Beyotime). The concentrations of total protein were quantified as described above. Protein samples were next separated by 8%, 12%, 15% (chosen by protein molecular weight) sodium dodecyl sulfate-polyacrylamide gel electrophoresis (SDS-PAGE) gel and transferred onto polyvinylidene fluoride (PVDF, LC2005, ThermoFisher, MA, USA) membranes

at 80V for 1.5 h. Membranes were blocked with 5% BSA (1 h at RT) and then incubated with primary antibodies at 4°C overnight: HDAC5 (1:1000, 16166-1-AP, Proteintech Group, Wuhan, China), HIF-1α (1:1000, 20960-1-AP, Proteintech Group), VEGFA (1:1000, DF7470, Affinity Bioscience, Jiangsu, China), p-VEGFR2 (1:1000, AF4426, Affinity Bioscience), VEGFR2 (1:500, sc-393163, Santa Cruz Biotech, Santa Cruz, CA, USA) and β-actin (1: 2000, 60008-1-Ig, proteintech Group). After washing, membranes were next probed with secondary antibody (1:10000, SA00001-1, SA00001-2, Proteintech Group) for 40 min at 37°C. The representative blots were further visualized using enhanced chemiluminescence substrate (ECL) solution (P0018S, Beyotime), and quantified by the software of Gel-Pro-Analyzer (Media Cybernetics, Rockville, MD, USA). β-actin was used as an internal control. The quantitative analysis of our target proteins was conducted by being normalized to β-actin.

Co-immunoprecipitation. Ovarian protein extracts from each group were immuno-precipitated with indicated antibodies at 4°C overnight to form antigen-antibody complexes. Subsequently, previously rinsed protein-A-agarose beads were added to the complex and maintained for 2 h at 4°C. After three-time washing with cold phosphate-buffered saline (PBS), the protein was eluted by loading buffer and boiled for 5 min. The supernatant was assigned to immunoblotting using Acetyl-Lysine antibody (1:500, A2391, ABclonal, Wuhan, China), VEGFR2 (1:500, sc-393163, Santa Cruz Biotech) and HDAC5 antibody (1:1000, 16166-1-AP, Proteintech Group).

Statistical analysis. All data were presented as mean ± standard deviation (SD). Our data met with normal distribution, and parametric tests were used in this study. One-way analysis of variance (one-way ANOVA) followed by Tukey's test was used for comparison between multiple groups. All statistical analyses were performed by Graphpad Prism v. 8.0 (GraphPad Software, San Diego, CA, USA) and P-value of less than 0.05 was considered significant.

Results

HDAC5 improved pathological symptoms in DHEA-induced PCOS mice

As shown in Fig. 1A, PCOS was induced in female C57BL/6 mice by daily subcutaneous DHEA injections. HDAC5 over-expression *in vivo* was achieved by adenovirus administration. Ovaries in the PCOS group showed decreased number of corpora lutea (CLs), increased amounts of cystic follicles (CFs), and thinner granulosa cell layer when compared to control ones, while HDAC5 over-expression remarkably alleviated these PCOS symptoms (Fig. 1B). Besides, HDAC5 reduced serum levels of progesterone, testosterone, and estradiol, which were significantly augmented after PCOS modeling (Fig. 1C–E). The expression level of HDAC5 was respectively determined by real-time PCR and Western blotting. Accordingly, the compensatory increase in HDAC5 expression both at mRNA and protein levels was found in the ovaries of PCOS mice, and it was further augmented in PCOS + Ad-HDAC5 group (Fig. 1F–H).

HDAC5 inhibited angiogenesis in ovaries of DHEA-induced PCOS mice

To explore the effect of HDAC5 on ovarian angiogenesis in PCOS, the levels of several key angiogenesis-related factors, including VEGFA, PDGFB, PDGFD, ANGPT1, and ANGPT2, were analyzed in each experimental group. As shown in Fig. 2A, VEGFA mRNA level was notably increased in PCOS group and reversely decreased after HDAC5 over-expression. Additionally, HDAC5 inhibited the production of VEGFA and ANGPT1 in the ovaries of PCOS mice, while facilitating the generation of PDGFB, PDGFD, and ANGPT2 (Fig. 2B–F). It was further observed that CD31 positive staining was increased in ovarian vessels of PCOS mice and decreased after HDAC5 over-expression (Fig. 2G). Taken together, HDAC5 suppressed the excessive angiogenesis in ovaries of DHEA-induced PCOS mice.

HDAC5 suppressed oxidative stress in ovaries of DHEA-induced PCOS mice

As indicated in Fig. 3A–B, PCOS mice showed dramatically elevated levels of ROS and MDA in their ovaries, while HDAC5 reversed these changes. Meanwhile, HDAC5 was found to evidently enhance activities of CAT and SOD in ovaries of PCOS mice (Fig. 3C, D), which suggests that HDAC5 exerts an anti-oxidative effect in PCOS-mice ovaries.

HDAC5 inhibited HIF-1α/VEGF/VEGFR2 signaling in ovaries of DHEA-induced PCOS mice

The angiogenesis-related HIF-1α/VEGF/VEGFR2 signaling was further investigated in different experimental groups. As shown in Fig. 4A–B, protein levels of HIF-1α, VEGFA, p-VEGFR2, and VEGFR2 were significantly decreased after HDAC5 over-expression in the PCOS group, suggesting the inhibitory role of HDAC5 in HIF-1α/VEGF/VEGFR2 signaling. Besides, HDAC5 down-regulated the transcription levels of HIF-1α and VEGFR2 in ovaries of PCOS mice (Fig. 4C). Co-immunoprecipitation analysis indicated that HDAC5 interacted with VEGFR2 in ovaries of PCOS mice, and inhibited the acetylation of VEGFR2 (Fig. 4D, E), which has been reported to positively regulate VEGFR2 phosphorylation and receptor activity [24]. In summary, HDAC5 suppressed the

Folia Histochem Cytobiol. 2022
10.5603/FHC.a2022.0024
ISSN 0239-8508, e-ISSN 1897-5631

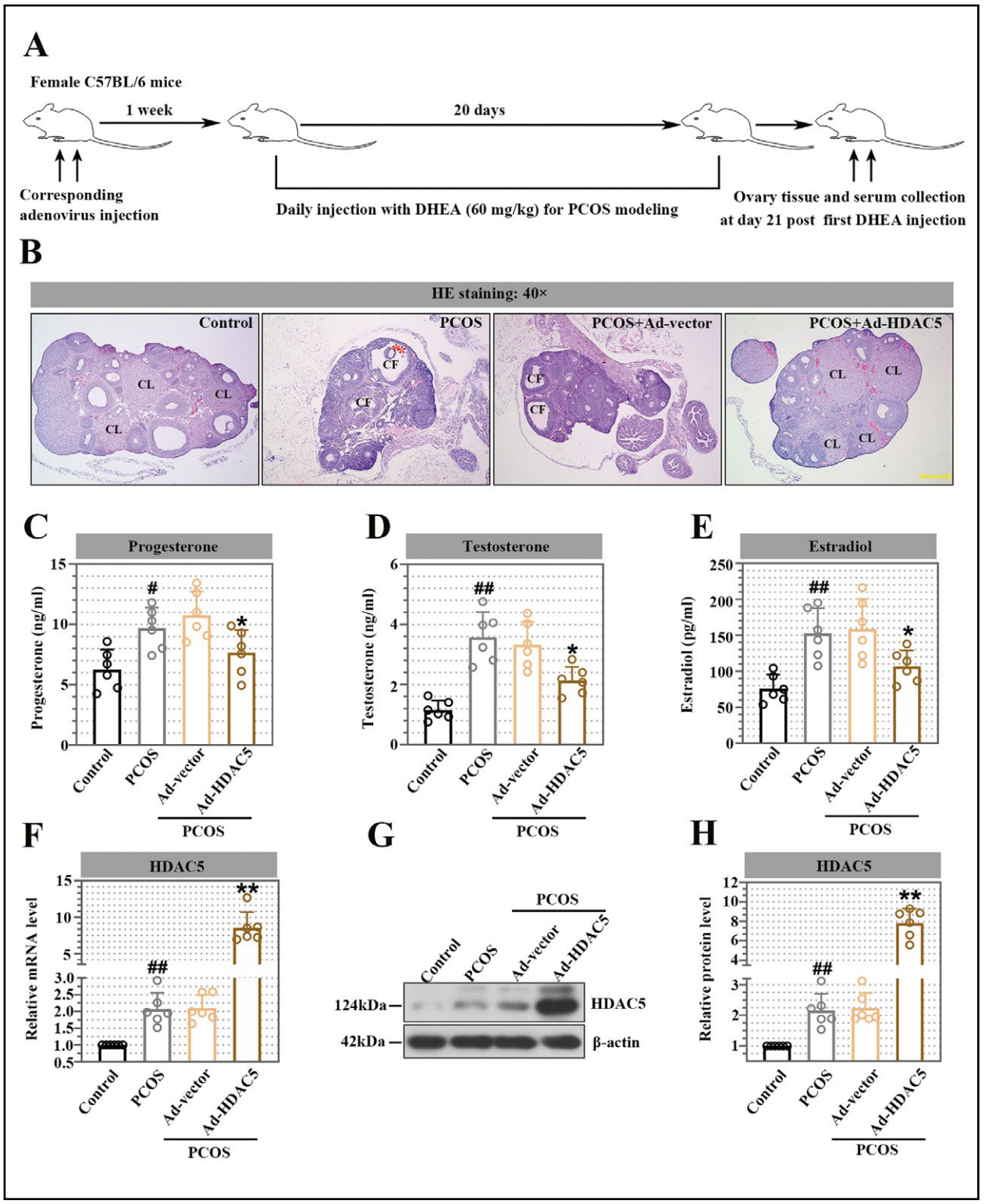

Figure 1. HDAC5 improved pathological symptoms in DHEA-induced polycystic ovary syndrome (PCOS) in mice. **A.** Brief flow chart of animal experiment. In young female mice, PCOS was induced by dehydroepiandrosterone (DHEA) administration (PCOS group). Some of the PCOS mice received injection of empty adenovirus (PCOS + Ad-vector group), whereas other PCOS mice received adenovirus expressing HDAC5 (PCOS + Ad-HDAC5 group). **B.** Ovarian morphology in each studied mouse group was determined by H&E staining at the magnification of 40×. Abbreviations: CL — corpus luteum; CF — cystic follicle. **C–E.** Serum levels of progesterone (C), testosterone (D) and estradiol (E) were detected by ELISA. **F–H.** mRNA and protein level of HDAC5 in ovary tissue of mice was measured by real-time PCR and Western blotting. Data was expressed as means ± SD (n = 6 in each group). $^{\#, \#\#}$ $P < 0.05$ and $P < 0.01$, respectively *vs.* control group; $^{*, **}$ $P < 0.05$ and $P < 0.01$, respectively, *vs.* PCOS + Ad-vector group.

Folia Histochem Cytobiol. 2022
10.5603/FHC.a2022.0024
ISSN 0239-8508, e-ISSN 1897-5631

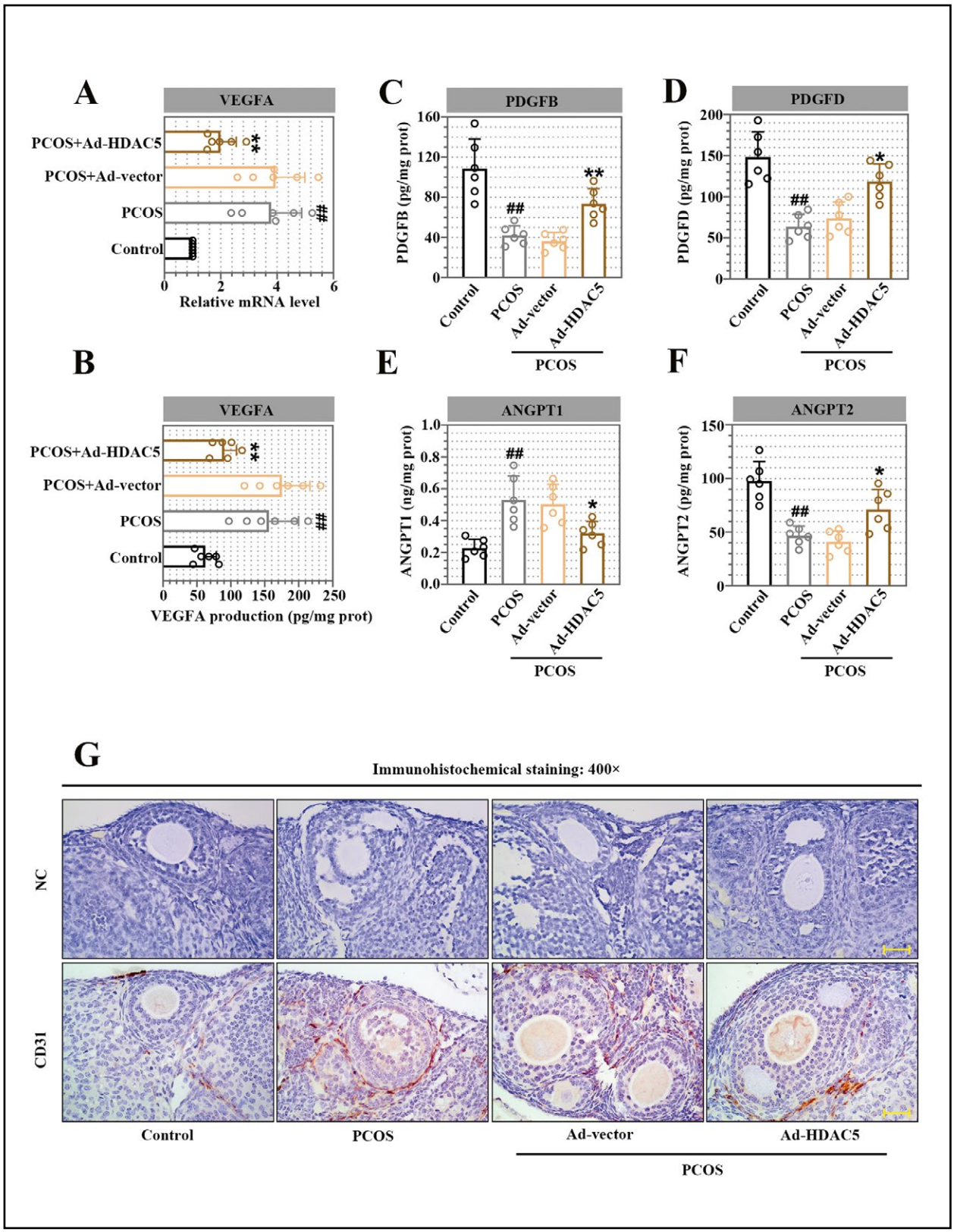

Figure 2. HDAC5 inhibited angiogenesis in ovaries of DHEA-induced PCOS mice. **A.** Relative mRNA levels of VEGFA in ovaries from each group of mice. **B–F.** Contents of VEGFA (B), PDGFB (C), PDGFD (D), ANGPT1 (E) and ANGPT2 (F) in ovaries from each group of mice were determined by ELISA. **G.** The positive staining of CD31 was determined by immunohistochemistry. The allotypic serum was used as negative control to determine the specificity of CD31 staining. Magnification: 400×. Data was expressed as means ± SD (n = 6 in each group). Description of experimental groups as in the legend to Fig. 1. $^{\#, \#\#}$ $P < 0.05$ and $P < 0.01$, respectively *vs.* control group; $^{*, **}$ $P < 0.05$ and $P < 0.01$, respectively, *vs.* PCOS + Ad-vector group.

Folia Histochem Cytobiol. 2022
10.5603/FHC.a2022.0024
ISSN 0239-8508, e-ISSN 1897-5631

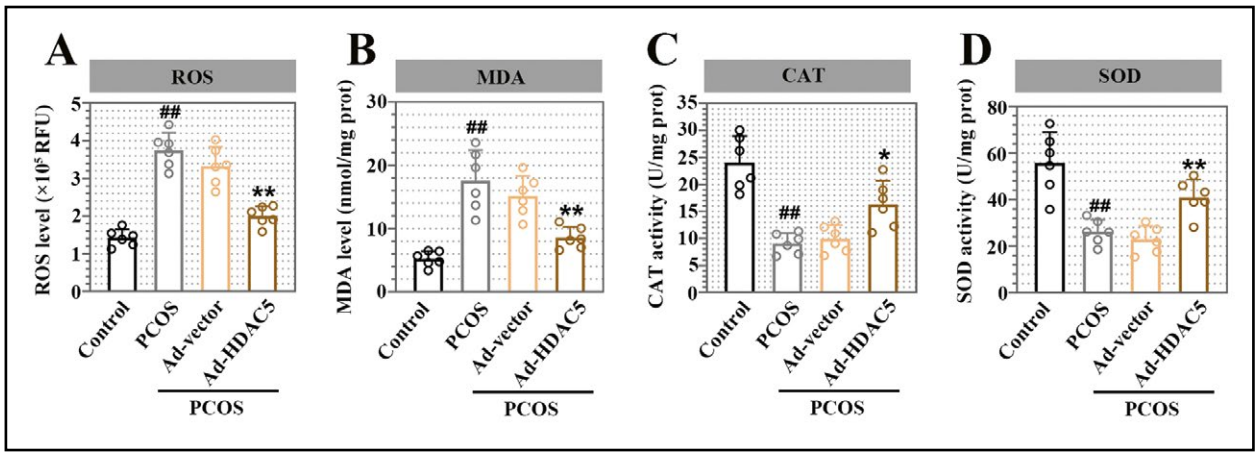

Figure 3. HDAC5 suppressed oxidative stress in ovaries of DHEA-induced PCOS mice. **A.** ROS level in each group was measured by flow cytometric analysis using DCFH-DA probe. **B–D.** The malondialdehyde (MDA) levels (B), catalase (CAT) activity (C) and superoxide dismutase (SOD) activity (D) were measured as described in Methods. Data was expressed as means ± SD (n = 6 in each group). $^{\#, \#\#}$ $P < 0.05$ and $P < 0.01$, respectively *vs.* control group; $^{*, **}$ $P < 0.05$ and $P < 0.01$, respectively, *vs.* PCOS + Ad-vector group.

activation of angiogenesis-related HIF-1α/VEGF/ /VEGFR2 signaling in ovaries of PCOS mice (Fig. 4F).

Discussion

PCOS is acknowledged as a heterogeneous endocrine disease characterized by obvious ovarian dysfunction. The pathogenesis of PCOS is complex and waits for further investigation. Growing evidence has suggested the key role of ovarian angiogenesis in PCOS development. Herein, we propose the protective effect of HDAC5 on PCOS progression *via* inhibiting ovarian angiogenesis.

In this study, PCOS was induced in mice by the administration of DHEA, a well-established method for PCOS modeling [25]. The altered ovarian morphology, as evidenced by decreased CL and increased cystic structures, was observed in DHEA-treated mice, suggesting the abnormal follicular development in ovaries of PCOS mice. Ovarian follicles are the basic functional units of ovaries. They provide proper environments for oocyte growth and development, which are crucial early events for ovulation and fertilization [26]. Besides, PCOS is believed to be a prevalent hormonal disorder among premenopausal women and it is generally featured with high levels of androgen [27]. Consistently with previous research, DHEA in this study induced statistical elevation of several serum hormones in PCOS mice, such as testosterone, a characteristic parameter of PCOS [28]. More interestingly, a compensatory increase in HDAC5 expression was found in PCOS ovaries and its over-expression significantly alleviated these abnormalities in PCOS mice, suggesting the protective role of HDAC5 in PCOS.

Increasing evidence has validated the occurrence of excessive angiogenesis during PCOS development, which is likely to result in impaired follicular development and defective fertility in PCOS patients [29]. Thus, we further investigate the effect of HDAC5 on ovarian angiogenesis in PCOS, and it turned out that HDAC5 significantly inhibited DHEA-induced angiogenesis in PCOS mice by regulating angiogenesis-related factors, such as VEGFA, PDGFB/D, ANGPT1/2, and CD31. VEGFA is the most investigated member of the VEGF family, and it has been linked to angiogenesis for regulating vascular endothelial cell proliferation and migration [30]. Besides, the increased concentration of VEGF has been reported in the ovaries of PCOS women since 1995 [31]. PDGFB/D and ANGPT1/2 respectively belong to the family of platelet-derived growth factor (PDGF) and angiopoietin (ANGPT), and they mainly regulate the maturity, stability, and permeability of vessels during the angiogenic process [5, 32]. Thereinto, ANGPT1 facilitates the formation of new vessels, while increased ANGPT2 leads to vascular destabilization and regression [5]. Regarding PDGFB and PDGFD, they are critical factors for vessel maturation, and their abundances are significantly decreased in the ovaries of DHEA-treated rats and follicular fluids of PCOS individuals [5, 32, 33]. In regard to CD31, it is a classical marker of vascular endothelial cells and has been considered as an important indicator for angiogenesis. It is worthy to note that HDAC5 over-expression in this study remarkedly decreased the expression of VEGFA, ANGPT1 and CD31, while facilitating the generation of PDGFB, PDGFD, and ANGPT2 in ovaries of PCOS mice, which makes HDAC5 a novel regulator of ovarian angiogenesis in PCOS.

Folia Histochem Cytobiol. 2022
10.5603/FHC.a2022.0024
ISSN 0239-8508, e-ISSN 1897-5631

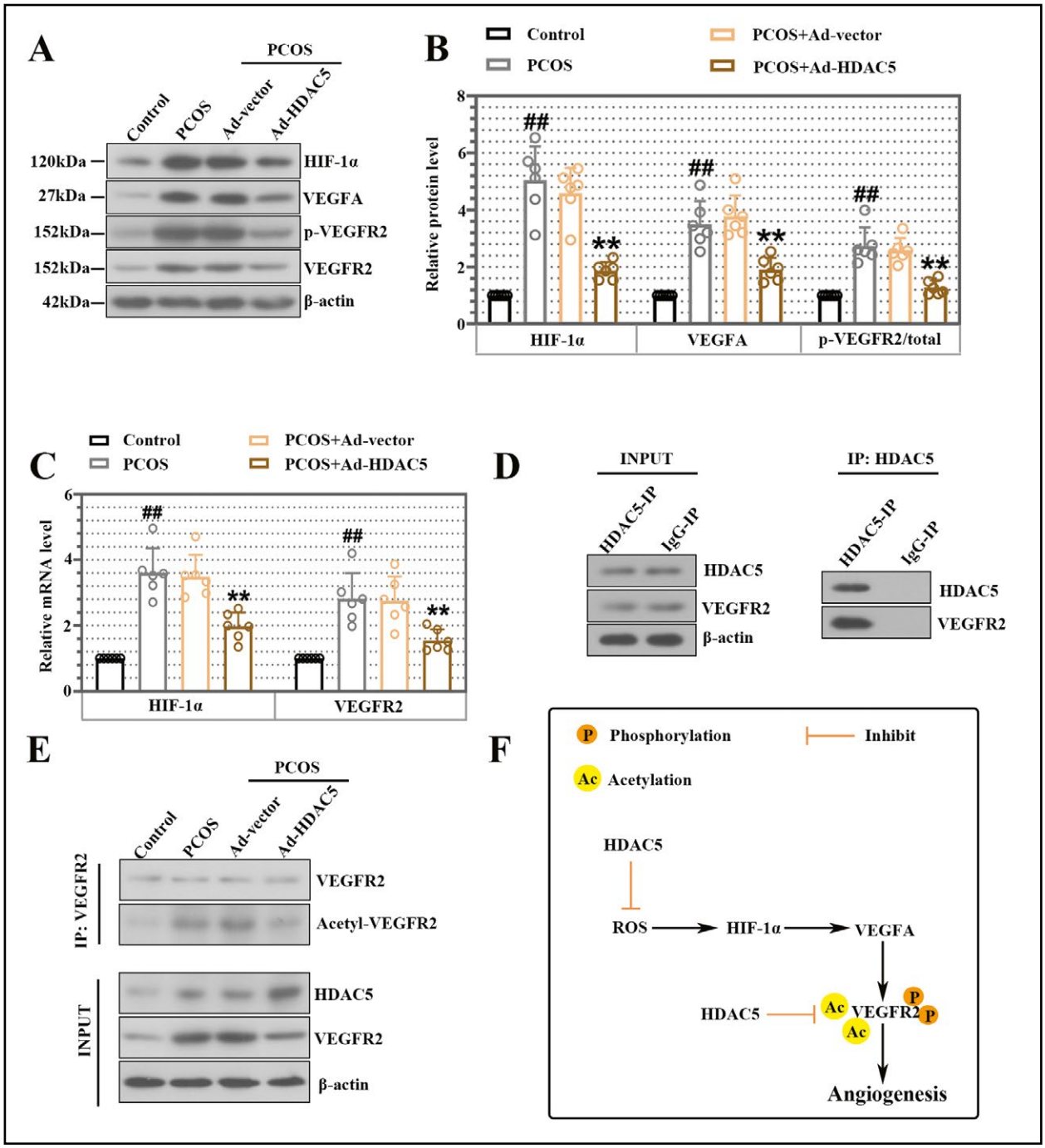

Figure 4. HDAC5 inhibited HIF-1α/VEGF/VEGFR2 signaling in ovaries of DHEA-induced PCOS mice. **A–B.** Western-blot analysis of the protein levels of HIF-1α, VEGFA, p-VEGFR2 (Tyr 1175) and VEGFR2. **C.** Real-time PCR analysis of the mRNA levels of HIF-1α and VEGFR2. **D.** Co-immunoprecipitation was performed to determine the interaction between HDAC5 and VEGFR2 in ovaries of PCOS mice with anti-HDAC5 antibody. **E.** Acetylation level of VEGFR2 in ovaries from each group of mice was determined by immunoprecipitation using anti-VEGFR2 antibody. **F.** Brief schematic presentation of the proposed effect of HDAC5 on angiogenesis. Data was expressed as means ± SD (n = 6 in each group). $^{\#, \#\#}$ $P < 0.05$ and $P < 0.01$, respectively *vs.* control group; $^{*, **}$ $P < 0.05$ and $P < 0.01$, respectively, *vs.* PCOS + Ad-vector group.

We further determined that HDAC5 inhibited oxidative stress in ovaries of PCOS mice, as evidenced by reduced ROS levels and enhanced activities of anti-oxidative enzymes. Consistent with our finding, excessive oxidative stress was documented in PCOS patients [34], and, thus, may be regarded as a promising target for PCOS therapy [35]. Moreover, oxidative stress is considered as a hallmark for many kinds of vascular diseases, and it contributes to the angiogenic process under several pathological states. In brief,

Folia Histochem Cytobiol. 2022
10.5603/FHC.a2022.0024
ISSN 0239-8508, e-ISSN 1897-5631

oxidative stress-induced angiogenesis is initiated by over-produced ROS and involves HIF-1α/VEGF/VEGFR2 signaling [14, 36].

VEGF is a key factor in angiogenesis, and HIF-1α is a transcription factor mainly targeting at VEGF gene during angiogenesis. HIF-1α expression is reported to be dramatically reduced in PCOS patients after the administration of resveratrol, an effective drug to improve PCOS [37, 38], which indicates the involvement of HIF-1α in PCOS. In this study, we found that HDAC5 remarkably reduced expression levels of HIF-1α, VEGFA, VEGFR2, and p-VEGFR2 in PCOS ovaries, suggesting the inhibitory effect of HDAC5 on HIF-1α/VEGFA/VEGFR2 signaling. It should be noted that this signaling functions upon the activation of VEGFR2. Generally, VEGFR2 undergoes phosphorylation after VEGFA stimulation, and it consequently leads to the initiation of downstream angiogenesis signaling [39]. More inspiringly, Zecchin *et al*. suggest that there exists crosstalk among VEGFR2 phosphorylation and its acetylation. VEGFR2 acetylation is elucidated to promote its phosphorylation and facilitates receptor activity in endothelial cells [24]. Consistent with previous research, HDAC5 was proved to inhibit VEGFR2 acetylation in ovaries of PCOS mice, suggesting that HDAC5 might regulate VEGFA/VEGFR2 signaling *via* its ability of deacetylation. As a representative histone deacetylase, HDAC5-mediated deacetylation has shown critical effects on breast cancer management [40]. HDAC5--induced p65 deacetylation participates in modulating cancer immunity and PD-L1 expression in pancreatic cancer [41]. Herein, in this study, we propose that HDAC5-induced VEGFR2 deacetylation might be implicated in ovarian angiogenesis in PCOS.

Nonetheless, our findings just indicated the simple inhibitory effects of HDAC5 on abnormal angiogenesis and HIF-1α/VEGFA/VEGFR2 signaling in DHEA-induced PCOS mice. However, we didn't fully explore whether HDAC5 regulated ovarian angiogenesis in PCOS mice *via* inhibiting HIF-1α/VEGFA/ /VEGFR2 signaling since lack of suitable activator targeting this signaling pathway for the rescue assay. Thus, our findings are subjected to some limitations and await further investigations.

In summary, this study reveals the compensatory increase of HDAC5 expression in ovaries of DHEA-induced PCOS mice. HDAC5 over-expression *in vivo* protects against ovarian angiogenesis and oxidative stress in PCOS mice. Additionally, this study further determines that HDAC5 inhibits the activation of angiogenesis-related HIF-1α/VEGFA/VEGFR2 signaling in ovaries of PCOS mice partly by its ability of deacetylation. Collectively, the results of this study suggest that HDAC5 could be a molecular candidate for PCOS intervention in the future.

Funding

This research was supported by grants from the National Natural Science Foundation of China (grant number: 81904235) and the Excellent Innovative Talents Program of Heilongjiang University of Chinese Medicine (grant number: 2018RCQ03).

Authors' contribution

YW, LH, and XF designed the experiment. YW, Yu W, YC, and QG performed the experiments and analyze the data. YW, LH, and XF wrote the manuscript. All authors read and approved the manuscript.

Conflict of interest

The authors declare no competing interests.

References

1. Zhang F, Ma T, Cui P, et al. Diversity of the gut microbiota in dihydrotestosterone-induced PCOS rats and the pharmacologic effects of diane-35, probiotics, and berberine. Front Microbiol. 2019; 10: 175, doi: 10.3389/fmicb.2019.00175, indexed in Pubmed: 30800111.
2. Mu Y, Cheng D, Yin TL, et al. Vitamin D and polycystic ovary syndrome: a narrative review. Reprod Sci. 2021; 28(8): 2110–2117, doi: 10.1007/s43032-020-00369-2, indexed in Pubmed: 33113105.
3. Ali AT, Guidozzi F, Ali AT. Polycystic ovary syndrome and metabolic syndrome. Ceska Gynekol. 2015; 80(4): 279–289, indexed in Pubmed: 26265416.
4. Di Pietro M, Pascuali N, Parborell F, et al. Metformin regulates ovarian angiogenesis and follicular development in a female polycystic ovary syndrome rat model. Endocrinology. 2015; 156(4): 1453–1463, doi: 10.1210/en.2014-1765, indexed in Pubmed: 25590243.
5. Wei J, Zhao Y. MiR-185-5p protects against angiogenesis in polycystic ovary syndrome by targeting VEGFA. Front Pharmacol. 2020; 11: 1030, doi: 10.3389/fphar.2020.01030, indexed in Pubmed: 32760272.
6. Tan BK, Adya R, Chen J, et al. Metformin decreases angiogenesis via NF-kappaB and Erk1/2/Erk5 pathways by increasing the antiangiogenic thrombospondin-1. Cardiovasc Res. 2009; 83(3): 566–574, doi: 10.1093/cvr/cvp131, indexed in Pubmed: 19414528.
7. Di Pietro M, Parborell F, Irusta G, et al. Metformin regulates ovarian angiogenesis and follicular development in a female polycystic ovary syndrome rat model. Endocrinology. 2015; 156(4): 1453–1463, doi: 10.1210/en.2014-1765, indexed in Pubmed: 25590243.
8. Xu Z, Jia K, Wang H, et al. METTL14-regulated PI3K/Akt signaling pathway via PTEN affects HDAC5-mediated epithelial-mesenchymal transition of renal tubular cells in diabetic kidney disease. Cell Death Dis. 2021; 12(1): 32, doi: 10.1038/s41419-020-03312-0, indexed in Pubmed: 33414476.

9. Johnstone RW. Histone-deacetylase inhibitors: novel drugs for the treatment of cancer. Nat Rev Drug Discov. 2002; 1(4): 287–299, doi: 10.1038/nrd772, indexed in Pubmed: 12120280.
10. Zhou Y, Jin X, Ma J, et al. HDAC5 loss impairs RB repression of pro-oncogenic genes and confers CDK4/6 inhibitor resistance in cancer. Cancer Res. 2021; 81(6): 1486–1499, doi: 10.1158/0008-5472.CAN-20-2828, indexed in Pubmed: 33419772.
11. Huang Y, Tan M, Gosink M, et al. Histone deacetylase 5 is not a p53 target gene, but its overexpression inhibits tumor cell growth and induces apoptosis. Cancer Res. 2002; 62(10): 2913–2922, indexed in Pubmed: 12019172.
12. Li B, Zhang L, Zhu L, et al. HDAC5 promotes intestinal sepsis via the Ghrelin/E2F1/NF-κB axis. FASEB J. 2021; 35(7): e21368, doi: 10.1096/fj.202001584R, indexed in Pubmed: 34125448.
13. Urbich C, Rössig L, Kaluza D, et al. HDAC5 is a repressor of angiogenesis and determines the angiogenic gene expression pattern of endothelial cells. Blood. 2009; 113(22): 5669–5679, doi: 10.1182/blood-2009-01-196485, indexed in Pubmed: 19351956.
14. Kim YW, Byzova TV, et al. Oxidative stress in angiogenesis and vascular disease. Blood. 2014; 123(5): 625–631, doi: 10.1182/blood-2013-09-512749, indexed in Pubmed: 24300855.
15. Zuo T, Zhu M, Xu W. Roles of oxidative stress in polycystic ovary syndrome and cancers. Oxid Med Cell Longev. 2016; 2016: 8589318, doi: 10.1155/2016/8589318, indexed in Pubmed: 26770659.
16. Hu T, Schreiter FC, Bagchi RA, et al. HDAC5 catalytic activity suppresses cardiomyocyte oxidative stress and NRF2 target gene expression. J Biol Chem. 2019; 294(21): 8640–8652, doi: 10.1074/jbc.RA118.007006, indexed in Pubmed: 30962285.
17. Shi L, Tian Z, Fu Q, et al. miR-217-regulated MEF2D-HDAC5/ND6 signaling pathway participates in the oxidative stress and inflammatory response after cerebral ischemia. Brain Res. 2020; 1739: 146835, doi: 10.1016/j.brainres.2020.146835, indexed in Pubmed: 32311345.
18. Abramovich D, Irusta G, Bas D, et al. Angiopoietins/TIE2 system and VEGF are involved in ovarian function in a DHEA rat model of polycystic ovary syndrome. Endocrinology. 2012; 153(7): 3446–3456, doi: 10.1210/en.2012-1105, indexed in Pubmed: 22577112.
19. Azhary JMK, Harada M, Kunitomi C, et al. Androgens increase accumulation of advanced glycation end products in granulosa cells by activating ER stress in PCOS. Endocrinology. 2020; 161(2), doi: 10.1210/endocr/bqaa015, indexed in Pubmed: 32020188.
20. Luo J, Deng ZL, Luo X, et al. A protocol for rapid generation of recombinant adenoviruses using the AdEasy system. Nat Protoc. 2007; 2(5): 1236–1247, doi: 10.1038/nprot.2007.135, indexed in Pubmed: 17546019.
21. Cardiff RD, Miller CH, Munn RJ. Manual hematoxylin and eosin staining of mouse tissue sections. Cold Spring Harb Protoc. 2014; 2014(6): 655–658, doi: 10.1101/pdb.prot073411, indexed in Pubmed: 24890205.
22. Reichard A, Asosingh K. Best practices for preparing a single cell suspension from solid tissues for flow cytometry. Cytometry A. 2019; 95(2): 219–226, doi: 10.1002/cyto.a.23690, indexed in Pubmed: 30523671.
23. Livak KJ, Schmittgen TD. Analysis of relative gene expression data using real-time quantitative PCR and the 2(-Delta Delta C(T)) Method. Methods. 2001; 25(4): 402–408, doi: 10.1006/meth.2001.1262, indexed in Pubmed: 11846609.
24. Zecchin A, Pattarini L, Gutierrez MI, et al. Reversible acetylation regulates vascular endothelial growth factor receptor-2 activity. J Mol Cell Biol. 2014; 6(2): 116–127, doi: 10.1093/jmcb/mju010, indexed in Pubmed: 24620033.
25. Emidio GDi, Placidi M, Rea F, et al. Methylglyoxal-Dependent glycative stress and deregulation of SIRT1 functional network in the ovary of PCOS mice. Cells. 2020; 9(1): 209, doi: 10.3390/cells9010209, indexed in Pubmed: 31947651.
26. Lim M, Thompson JG, Dunning KR. HYPOXIA AND REPRODUCTIVE HEALTH: Hypoxia and ovarian function: follicle development, ovulation, oocyte maturation. Reproduction. 2021; 161(1): F33–F40, doi: 10.1530/REP-20-0509, indexed in Pubmed: 33361508.
27. Zhang J, Bao Y, Zhou Xu, et al. Polycystic ovary syndrome and mitochondrial dysfunction. Reprod Biol Endocrinol. 2019; 17(1): 67, doi: 10.1186/s12958-019-0509-4, indexed in Pubmed: 31420039.
28. Tessaro I, Modina SC, Franciosi F, et al. Effect of oral administration of low-dose follicle stimulating hormone on hyperandrogenized mice as a model of polycystic ovary syndrome. J Ovarian Res. 2015; 8: 64, doi: 10.1186/s13048-015-0192-9, indexed in Pubmed: 26437930.
29. Di Pietro M, Scotti L, Irusta G, et al. Local administration of platelet-derived growth factor B (PDGFB) improves follicular development and ovarian angiogenesis in a rat model of Polycystic Ovary Syndrome. Mol Cell Endocrinol. 2016; 433: 47–55, doi: 10.1016/j.mce.2016.05.022, indexed in Pubmed: 27256152.
30. Laddha AP, Kulkarni YA. VEGF and FGF-2: Promising targets for the treatment of respiratory disorders. Respir Med. 2019; 156: 33–46, doi: 10.1016/j.rmed.2019.08.003, indexed in Pubmed: 31421589.
31. Kamat BR, Brown LF, Manseau EJ, et al. Expression of vascular permeability factor/vascular endothelial growth factor by human granulosa and theca lutein cells. Role in corpus luteum development. Am J Pathol. 1995; 146(1): 157–165, indexed in Pubmed: 7531945.
32. Pascuali N, Scotti L, Oubiña G, et al. Platelet-derived growth factor B restores vascular barrier integrity and diminishes permeability in ovarian hyperstimulation syndrome. Mol Hum Reprod. 2020; 26(8): 585–600, doi: 10.1093/molehr/gaaa038, indexed in Pubmed: 32467982.
33. Scotti L, Parborell F, Irusta G, et al. Platelet-derived growth factor BB and DD and angiopoietin1 are altered in follicular fluid from polycystic ovary syndrome patients. Mol Reprod Dev. 2014; 81(8): 748–756, doi: 10.1002/mrd.22343, indexed in Pubmed: 24889290.
34. Hilali N, Vural M, Camuzcuoglu H, et al. Increased prolidase activity and oxidative stress in PCOS. Clin Endocrinol (Oxf). 2013; 79(1): 105–110, doi: 10.1111/cen.12110, indexed in Pubmed: 23163753.
35. Ostadmohammadi V, Jamilian M, Bahmani F, et al. Vitamin D and probiotic co-supplementation affects mental health, hormonal, inflammatory and oxidative stress parameters in women with polycystic ovary syndrome. J Ovarian Res. 2019; 12(1): 5, doi: 10.1186/s13048-019-0480-x, indexed in Pubmed: 30665436.
36. Xian D, Song J, Yang L, et al. Emerging roles of redox-mediated angiogenesis and oxidative stress in dermatoses. Oxid Med Cell Longev. 2019; 2019: 2304018, doi: 10.1155/2019/2304018, indexed in Pubmed: 31178954.
37. Liang A, Huang L, Liu H, et al. Resveratrol improves follicular development of PCOS rats by regulating the glycolytic pathway. Mol Nutr Food Res. 2021; 65(24): e2100457, doi: 10.1002/mnfr.202100457, indexed in Pubmed: 34664388.
38. Bahramrezaie M, Amidi F, Aleyasin A, et al. Effects of resveratrol on VEGF & HIF1 genes expression in granulosa cells in the angiogenesis pathway and laboratory parameters of polycystic ovary syndrome: a triple-blind randomized clinical trial. J Assist Reprod Genet. 2019; 36(8): 1701–1712, doi: 10.1007/s10815-019-01461-6, indexed in Pubmed: 31327131.

Folia Histochem Cytobiol. 2022
10.5603/FHC.a2022.0024
ISSN 0239-8508, e-ISSN 1897-5631

39. Parma L, Peters HAB, Johansson ME, et al. Bis(maltolato)oxovanadium(IV) Induces Angiogenesis via Phosphorylation of VEGFR2. Int J Mol Sci. 2020; 21(13), doi: 10.3390/ijms21134643, indexed in Pubmed: 32629855.
40. Xue Y, Lian W, Zhi J, et al. HDAC5-mediated deacetylation and nuclear localisation of SOX9 is critical for tamoxifen resistance in breast cancer. Br J Cancer. 2019; 121(12): 1039–1049, doi: 10.1038/s41416-019-0625-0, indexed in Pubmed: 31690832.
41. Zhou Y, Jin X, Yu H, et al. HDAC5 modulates PD-L1 expression and cancer immunity via p65 deacetylation in pancreatic cancer. Theranostics. 2022; 12(5): 2080–2094, doi: 10.7150/thno.69444, indexed in Pubmed: 35265200.

Submitted: 15 May, 2022
Accepted after reviews: 17 August, 2022
Available as AoP: 16 September, 2022